

# An Optimized Enzyme-Nucleobase Pair Enables *In Vivo* RNA Metabolic Labeling with Improved Cell-Specificity

Monika K. Singha, Jan Zimak, Samantha R. Levine, Nan Dai, Chan Hong, Cecily Anaraki, Mrityunjay Gupta, Christopher J. Halbrook, Scott X. Atwood, and Robert C. Spitale\*



Cite This: *Biochemistry* 2022, 61, 2638–2642



Read Online

ACCESS |



Metrics & More



Article Recommendations



Supporting Information

**ABSTRACT:** Current transcriptome-wide analyses have identified a growing number of regulatory RNA with expression that is characterized in a cell-type-specific manner. Herein, we describe RNA metabolic labeling with improved cell-specificity utilizing the *in vivo* expression of an optimized uracil phosphoribosyltransferase (UPRT) enzyme. We demonstrate improved selectivity for metabolic incorporation of a modified nucleobase (5-vinyuracil) into nascent RNA, using a battery of tests. The selective incorporation of vinyl-U residues was demonstrated in 3xUPRT LM2 cells through validation with dot blot, qPCR, LC-MS/MS and microscopy analysis. We also report using this approach in a metastatic human breast cancer mouse model for profiling cell-specific nascent RNA.

During the past decade, RNA have been recognized as macromolecules with diverse biological functions important in distinctive cell-type specific processes.<sup>1</sup> Identifying regulatory RNA in a specific cell-type remains particularly challenging within *in vivo* experimental models due to the presence of many cell-types. To capture RNA from cell-types of interest, extensive dissociation and isolation steps are required prior to isolating RNA for analysis.<sup>2</sup> These approaches rely on mechanical separation, enzymatic digestion and flow cytometry, which are all known to introduce transcriptional artifacts, as the cellular transcriptome is transformed when the cells are removed from the original whole-organism environmental niche.<sup>3</sup> Recapitulation of RNA expression pathways from intact, living cells within model organisms is difficult to analyze with these current techniques due to these challenges.

RNA metabolic labeling methods tag nascent RNA within living cells, which provides opportunities for capturing transcriptional information present during key biological events. These methods expose cells to noncanonical nucleobase or nucleosides derivatized with chemical handles for subsequent metabolic incorporation into newly polymerizing RNA.<sup>4</sup> Isolation of total RNA includes a portion of metabolically tagged nascent transcripts that are reactive to biotin-conjugated, orthogonal chemical reagents for subsequent streptavidin affinity-based enrichment and analysis. Attenuating RNA metabolic labeling to specific cell-types is achieved by expressing exogenous metabolic enzymes not active in mammalian cells that will selectively catalyze nucleobase analogs.

Our lab has demonstrated cell-specific RNA metabolic labeling with uracil phosphoribosyltransferase (UPRT) expression (from *Toxoplasma gondii*), TgUPRT, paired with 5-ethynyluracil (5-eu) consisting of a more stable, bioorthogonal chemical handle for imaging experiments with fluorophores and biochemical affinity-based separation of nascent tran-

scripts.<sup>5,6</sup> RNA labeled with ethynyl groups reacts with biotin-azide through Cu(I)-catalyzed azide-alkyne cycloaddition (CuAAC) that is known to deteriorate RNA integrity due to the production of metal-ion radicals.<sup>7</sup> Recent findings identified endogenous metabolic enzymes in the *de novo* pyrimidine biosynthetic pathway, notably uridine monophosphate synthase (UMPS), that are capable of catalyzing 5-eu in mammalian cell-types independent of UPRT expression limiting the applications for *in vivo* cell-specific RNA metabolic labeling.<sup>8</sup> These results necessitated the development of a more stringent enzyme-analog pair appropriate for cell-specific RNA metabolic labeling by the elimination of background, nonspecific RNA labeling in other cell-types.

To overcome challenges with 5-eu background RNA metabolic labeling in other mammalian cell-types, the active site of TgUPRT was engineered to generate triple mutant TgUPRT (3xUPRT) capable of catalyzing 5-vinyuracil (5-vu) into nascent, vinyl-labeled RNA without background labeling in wild-type cells (Figure 1a–c).<sup>9</sup> Advantages of using 5-vu include increased cell-specific stringency of labeling, as 5-vu is not recognized as a metabolic substrate by UMPS.<sup>9</sup> Additionally, the vinyl handle reacts selectively with tetrazines through an inverse electron-demand Diels–Alder reaction which does not affect RNA integrity.<sup>9</sup> Finally, 5-vinyluridine (5-vuD) treatment in cells is shown to be less detrimental to cell proliferation at longer incubation times compared with 5-ethynyluridine for RNA metabolic labeling applications in cells

**Received:** September 26, 2022

**Revised:** November 10, 2022

**Published:** November 16, 2022



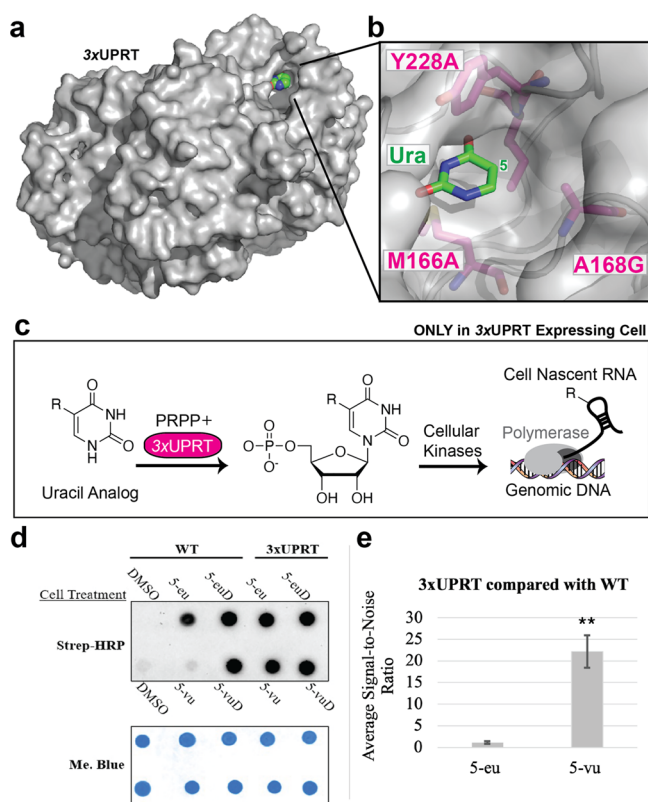


**Figure 1.** Characterizing cell-specific RNA metabolic labeling in MDA-MB-231 LM2 cells. 3-h cell treatment with 1 mM of DMSO (negative control), uracil analog, or uridine analog (positive control) in WT or (+)-3xUPRT cell lines. (a) Crystal structure of TgUPRT enzyme (PDB 1bd4). (b) Close-up view of TgUPRT active site. Positions chosen for mutagenesis are labeled. (c) Schematic of (–) TgUPRT versus TgUPRT expressing cells that enable cell-specific metabolic labeling of RNA. (d) RNA dot blot is performed after reacting with biotin-azide (for ethynyl RNA) or biotin-tetrazine (for vinyl RNA). RNA was cross-linked to membrane and incubated with streptavidin-horseradish peroxidase (Strep-HRP) followed by staining with methylene blue (Me-Blue) as a loading control. 5-eu = 5-ethynyluracil, 5-euD = 5-ethynyluridine, 5-vu = 5-vinyluracil, 5-vuD = 5-vinyluridine. (e) ImageJ quantification of chemiluminescence was used to calculate signal-to-noise ratios. Statistical significance relative to the WT signal was determined using a one-tailed Student's *t* test indicated as follows: *P* < 0.01; \*\*.

treated with each analog for >12 h.<sup>10</sup> These findings support use of the 3xUPRT enzyme paired with 5-vu for improved cell-type-specific RNA labeling within a broad range of applications in animal models and for maintaining the level of RNA integrity necessary for downstream sequencing analysis of enriched, labeled transcripts.

We predicted the 3xUPRT/5-vu cell-specific RNA labeling approach would be advantageous for profiling RNA in animal models where it is difficult to capture nascent RNA expression within specific cell-types without inducing transcriptional artifacts. Additionally, these technical improvements improve the flexibility of these protocols to include longer incubations beyond a few minutes and at higher concentrations which could be necessary in the larger context of a whole organism for labeling a specific cell population. To test this, 3xUPRT was stably and constitutively expressed in highly metastatic MDA-MB-231 LM2 (LM2) cells using CRISPR/Cas9 genome editing.<sup>11</sup> LM2 human breast cancer cells have shown

preferential metastasis into the lungs of mouse xenograft models without overburdening mice with the primary tumor size.<sup>12</sup> Before applying this approach into mice, cell-specific RNA metabolic labeling was characterized with dot blot analysis in cell culture experiments. The LM2 wild-type (WT) and (+)-3xUPRT cells were incubated with 5-eu or 5-vu at 1 mM for 3 h. As a positive control for RNA metabolic labeling, 5-ethynyluridine (5-euD) and 5-vinyluridine (5-vuD) were included in these experiments, which both label RNA in all cells regardless of 3xUPRT expression. Finally, DMSO was used as a negative control in cell treatments as the solvent of choice for these water-insoluble molecules. The extent of RNA labeling was measured from RNA isolated from each cell treatment with dot blot analysis (Figure 1d). The chemiluminescent signal from these dot blots was quantified with ImageJ to compare the differences in signal-to-noise between 5-eu and 5-vu treatments in (+)-3xUPRT LM2 cells compared with WT cells. These results showed a significantly higher signal-to-noise ratio with 5-vu treatment in (+)-3xUPRT cells when compared to 5-eu treatment in (+)-3xUPRT due to the prevalent background labeling in WT cells treated with 5-eu (Figure 1e). To verify 3xUPRT expression in LM2 cells, mCherry was coexpressed with 3xUPRT, whereas GFP is expressed in all the LM2 cell-types in this study (Figure S6).<sup>12</sup>

Prior to establishing mouse xenografts, optimization for *in vivo* RNA metabolic labeling protocols were tested in (WT) C57BL/6 mice. Rigorous testing of the solubility for these compounds in DMSO was shown to be maximized at 500 mM and resulted in using this concentration for intraperitoneal (IP) injections. Initially, 5-vinyluridine (5-vuD) was tested in two sets of WT mice, which demonstrated strong reproducibility of labeling across different tissue types depicted with RNA dot blot analysis, except for the brain due to low penetrance of the blood-brain barrier (Figure S1). Next, RNA labeling was performed in mice treated with uracil analogs, 5-eu and 5-vu, with uridine analogs, 5-euD and 5-vuD, as positive controls. These results clearly indicated stronger background labeling with 5-eu treatment compared with 5-vu over a 24-h treatment period, supporting that 5-vu is advantageous for improved cell-specificity of RNA labeling in mice (Figure S2).

In order to determine the range of background labeling with 5-vu, two biological replicates of WT mice were tested with increasing time points and number of injections, after which organs were surveyed with RNA dot blot analysis. Although the pancreas-derived RNA was extensively degraded due to high concentrations of endonucleases,<sup>13</sup> the majority of the RNA was compared effectively with this study to conclude that single-injection treatments at 1 h have significantly reduced background labeling compared to >5-h time points with >2 injections (Figure S3). Although the source of 5-vu background labeling was not investigated, we chose the 3-h time point and 500 mM injection [5-vu dose is 150 mg/kg and 5-vuD dose is 300 mg/kg] for testing the cell-specificity of RNA labeling in mouse tumor xenografts.

Using the stable LM2 WT (negative control) and (+)-3xUPRT cells, mouse xenografts were generated through mammary-fat pad implantation into NSG female mice. After 3–4 weeks, tumors were visible and mice were treated for 3 h with 500 mM 5-eu or 5-vu in triplicate. 5-euD and 5-vuD were each used as positive control treatments into one replicate mouse with WT LM2 tumors. After mice were sacrificed, tumor and organ RNA were isolated and reacted with biotin-tetrazine and then analyzed with RNA dot blot to determine

the extent of labeling (Figures 2a and S4). The signal-to-noise ratios of the chemiluminescent signal in mouse xenografts were

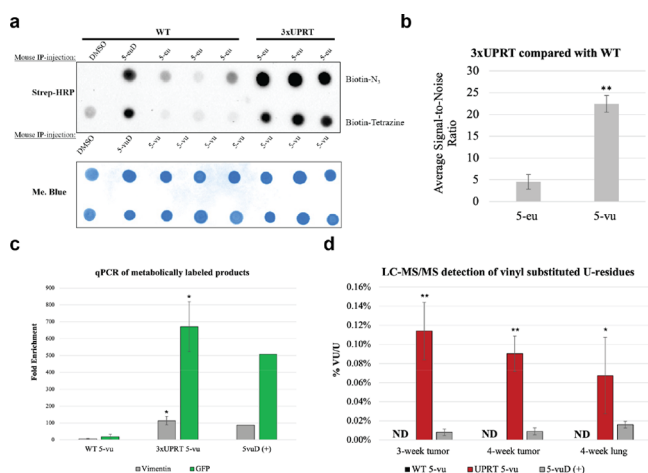


**Figure 2.** Cell-specific RNA metabolic labeling in mouse xenograft WT and (+)-3xUPRT LM2 primary tumors. The 3-week xenografted mice were IP-injected with 500 mM of each indicated substance for 3 h, including uracil analog treatments ( $n = 3$ ). (a) RNA was extracted from tumors and reacted with biotin- $N_3$  with ethynyl-RNA and biotin-tetrazine with vinyl-RNA prior to dot blot analysis. (b) ImageJ quantification of chemiluminescence was used to calculate signal-to-noise ratios. Statistical significance relative to the WT signal was determined using a one-tailed Student's  $t$  test indicated as follows:  $P < 0.01$ ; \*\*, 5-eu = 5-ethynyluracil, 5-euD = 5-ethynyluridine, 5-vu = 5-vinyluracil, 5-vuD = 5-vinyluridine. (c) Streptavidin bead enrichment of biotin-RNA:cDNA for qPCR analysis. Biotinylated RNA was reverse transcribed to make intact RNA:cDNA which were subsequently enriched with streptavidin beads, eluted by RNase hydrolysis and quantified with qPCR. Fold enrichment was determined through  $2^{-\Delta\Delta CT}$  standardized to the untreated mouse for vimentin and GFP labeled RNA. Statistical significance relative to enrichment from untreated mice was determined using a one-tailed Student's  $t$  test indicated as follows:  $P < 0.1$ ; \*, WT = wild-type, UPRT = 3xUPRT, 5-vu = 5-vinyluracil, 5vuD = 5-vinyluridine. (d) LC-MS/MS for analysis of vinyl-U modification from tumors and metastatic lungs. Purified RNA was analyzed for % of vinyl-U substitution of total U normalized to untreated mouse tissue. 3-week xenograft mouse lungs did not produce metastases and were not included in the analysis. Biological triplicates were used in this data set. Statistical significance relative to WT tumors and metastases was determined using a one-tailed Student's  $t$  test indicated as follows:  $P < 0.05$ ; \*\*,  $P < 0.5$ ; \*, WT = wild-type, UPRT = 3xUPRT, 5-vu = 5-vinyluracil, 5vuD = 5-vinyluridine, ND = not detected.

lower with more variability across 5-eu treatments in WT tumors compared with 5-vu treatments with overall significantly greater signal-to-noise (Figure 2b). To determine if 5-vu background could be reduced to any extent, 2-fold reduced titrations were included in (+)-3xUPRT tumor-containing mice (Figure S5). *Ex vivo* mCherry fluorescence showed similar size and consistent expression of 3xUPRT across these tumors (Figure S5). Flow cytometry was used to quantify GFP fluorescence in all LM2 cells used within mouse xenografts and mCherry fluorescence to verify numbers of the (+)-3xUPRT positive cell populations prior to transplantation (Figure S6).

To quantify the biochemical enrichment of metabolically labeled transcripts from WT and (+)-3xUPRT tumors, RNA was subjected to reverse transcription after reaction with tetrazine-biotin. Bypassing the RNase-H step, RNA:cDNA hybrids were incubated with MyOne C1 streptavidin magnetic

beads for separation and subsequent elution of cDNA from beads by RNase hydrolysis and heat; eluted cDNA was quantified with qPCR. Endogenous vimentin, known to be highly expressed in MDA-MB-231 cells,<sup>14</sup> and GFP, which was exogenously expressed within all MDA-MB-231 LM2 cells<sup>12</sup> in these experiments, were both quantified with qPCR. Untreated mouse RNA was included as a negative control, and 5-vinyluridine treated WT tumors were used as a positive control for enrichment. The fold enrichment was calculated by  $2^{-\Delta\Delta CT}$  with normalization to the untreated mouse enrichment levels for each detected gene.<sup>8</sup> A minimum of 10-fold enrichment for both genes of interest was reproducibly detected in (+)-3xUPRT/5-vu treated tumor samples (Figure 2c).

To quantify vinyl-substituted RNA, LC-MS/MS was used to determine the level of vinyl-U relative to total-U in tumor and lung samples. Both WT and (+)-3xUPRT tumor RNA from 3-week and 4-week xenografts were quantified to determine % vinyl substitution in uridine residues with metabolic labeling. Due to appreciable levels of lung metastases detected in 4-week xenografts, only 4-week lung RNA was included in this analysis. The ratio of 5-vu/total uracil residues was used to determine the % vinyl substitution rates across biological triplicates. WT tumor- and lung-derived RNA from 5-vuD treated mice were used as a positive control. These samples were normalized to RNA from mouse tissues without any analog treatment (Figure 2d). The percent incorporation of 5-vu/total uracil residues is an average of 0.1%, which is remarkable considering *in vitro* vinyl-incorporation was 0.8% for 5-vuD<sup>10</sup> RNA labeling in cells that were subjected to higher local analog concentrations and incubation times compared with conditions in these mouse xenograft studies.

For imaging nascent RNA, tetrazine-Cy5 was used to conjugate nascent, vinyl labeled RNA in mouse tumor and lung tissue sections. Tumor sections show uniformity of mCherry expression, indicating cells with 3xUPRT expression. The 4-week lung sections demonstrate dispersed metastatic (+)-3xUPRT LM2 cells within lung tissue with the colocalization of the Cy5 signal, demonstrating the level of cell-specificity achieved when captured through confocal microscopy. No background signal was detected in WT tumor sections reacted with tetrazine-Cy5 or the surrounding cell-types in the lung tissue. Although the overall fluorescent dye signal was reduced in lung tissue compared to tumor tissue, this can be attributed to the lungs being further from the IP-injection site, which may have reduced the bioavailability of 5-vu. These results clearly show that only (+)-3xUPRT cells in mouse tissues label nascent RNA with 5-vu, which can be detected with tetrazine-Cy5. These findings support the utility for 3xUPRT/5-vu for *in vivo* imaging of cell-specific nascent RNA (Figure 3 and Figure S7).

The cell-specific RNA metabolic labeling method described herein has the potential to transform the ability to analyze nascent RNA *in vivo* using widely available laboratory techniques. The most technically challenging aspect involved is to generate the stable expression of 3xUPRT into cell-types of interest, which can be performed with CRISPR/Cas9 genome-editing strategies. Second, 5-vu, biotin-tetrazine, and Cy5-tetrazine are commercially available for researchers to independently access if they lack resources to synthesize these reagents. Lastly, through the expression of downstream gene-specific promoters, 3xUPRT expression labels RNA when a gene-of-interest is actively expressed, thereby extending the

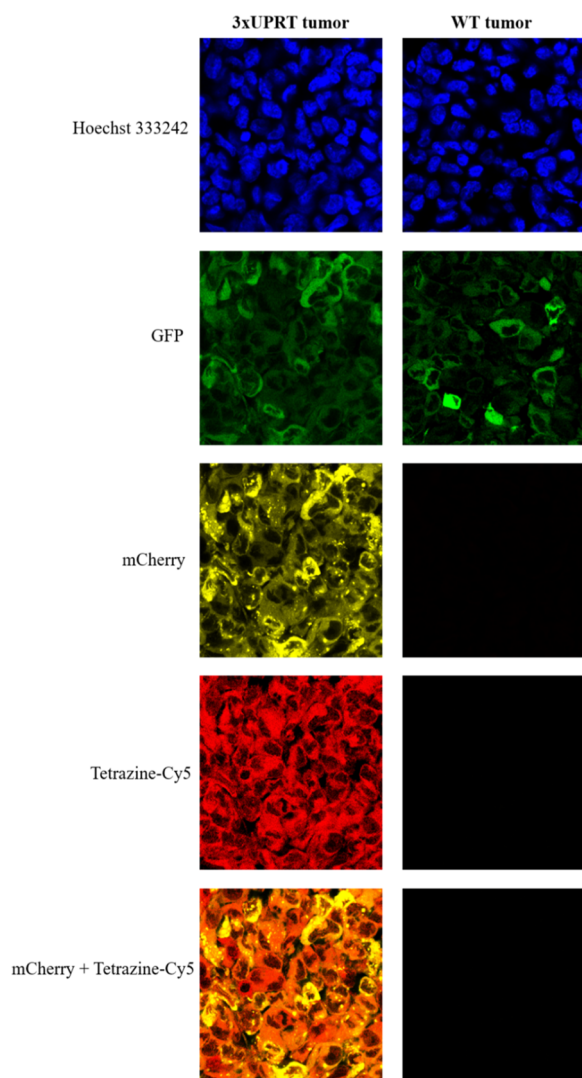


**Figure 3.** Metabolic labeling in (+)-3xUPRT-mCherry MDA-MB-231 LM2 cells in tumor tissues. Vinyl-containing RNA are fluorophore-conjugated with tetrazine-Cy5. GFP signal is present in WT MDA-MB-231 LM2 cells (parental line). mCherry signal indicates (+)-3xUPRT MDA-MB-231 cells.

utility of these tools to capture and visualize nascent RNA in a gene-specific and cell-specific context.

As a proof-of-principle, we generated MDA-MB-231 LM2 cells that stably express 3xUPRT driven by the endogenous vimentin promoter. We chose to generate vimentin-3xUPRT for the purpose of labeling RNA important for the maintenance of mesenchymal cell states, which occurs during the epithelial-to-mesenchymal transition in early metastatic progression<sup>14</sup> (Figure S8). The extent of labeling in vimentin-3xUPRT LM2 cells is overall comparable in chemiluminescent signal to the constitutively expressed (+)-3xUPRT LM2 cells used throughout this study and to the 5-vuD positive control signal. These exciting results support using this experimental approach for analyzing actively transcribed RNA pertinent to the epithelial-to-mesenchymal transition in greater detail by coexpressing 3xUPRT with other relevant genes and transcription factors of interest with the expectation of reduced nonspecific, background RNA labeling shown throughout this work.

In conclusion, these results have demonstrated the potential for researchers to design unique *in vivo* cell-specific RNA metabolic labeling experiments for model organisms of interest in order to elucidate complex transcriptional pathways in important cell-types.

## ■ ASSOCIATED CONTENT

### Supporting Information

The Supporting Information is available free of charge at <https://pubs.acs.org/doi/10.1021/acs.biochem.2c00559>.

IP-injection of 5-vuD (+) into WT mice, IP-injection with uracil and uridine analogs into WT mice, IP-injection of standard dose and 2-fold reduced dose in (+)-3xUPRT xenograft mice, flow cytometry analysis of WT and (+)-3xUPRT MDA-MB-231 LM2 cells prior to xenotransplantation, metabolic labeling in (+)-3xUPRT-mCherry MDA-MB-231 LM2 metastatic cells in lung tissues, RNA dot blot with vimentin-3xUPRT stable MDA-MB-231 cells, and experimental methods (PDF)

## ■ AUTHOR INFORMATION

### Corresponding Author

**Robert C. Spitale** – Department of Molecular Biology and Biochemistry, University of California, Irvine, Irvine, California 92697, United States; Department of Pharmaceutical Sciences and Department of Chemistry, University of California, Irvine, Irvine, California 92697, United States; [orcid.org/0000-0002-3511-8098](https://orcid.org/0000-0002-3511-8098); Email: [rspitale@uci.edu](mailto:rspitale@uci.edu)

### Authors

**Monika K. Singha** – Department of Molecular Biology and Biochemistry, University of California, Irvine, Irvine, California 92697, United States

**Jan Zimak** – Department of Pharmaceutical Sciences, University of California, Irvine, Irvine, California 92697, United States

**Samantha R. Levine** – Department of Pharmaceutical Sciences, University of California, Irvine, Irvine, California 92697, United States; [orcid.org/0000-0002-0496-9316](https://orcid.org/0000-0002-0496-9316)

**Nan Dai** – New England Biolabs, Beverly, Massachusetts 01915, United States

**Chan Hong** – Department of Cell and Developmental Biology, University of California, Irvine, Irvine, California 92697, United States

**Cecily Anaraki** – Department of Molecular Biology and Biochemistry, University of California, Irvine, Irvine, California 92697, United States

**Mrityunjay Gupta** – Department of Chemistry, University of California, Irvine, Irvine, California 92697, United States; [orcid.org/0000-0002-9118-1681](https://orcid.org/0000-0002-9118-1681)

**Christopher J. Halbrook** – Department of Molecular Biology and Biochemistry, University of California, Irvine, Irvine, California 92697, United States; [orcid.org/0000-0002-3376-3114](https://orcid.org/0000-0002-3376-3114)

**Scott X. Atwood** – Department of Cell and Developmental Biology, University of California, Irvine, Irvine, California 92697, United States

Complete contact information is available at: <https://pubs.acs.org/10.1021/acs.biochem.2c00559>

## Author Contributions

All authors have given approval to the final version of the manuscript.

## Funding

Spitale lab work in this manuscript is supported by the University of California, Irvine and the Pew Biomedical Scholar program (R.C.S.).

## Notes

The authors declare no competing financial interest.

## ACKNOWLEDGMENTS

We thank members of the Spitale lab for their careful reading and critique of the manuscript.

## ABBREVIATIONS

Strep-HRP, Streptavidin-Horseradish Peroxidase; Me-Blue, Methylene Blue; 5-eu, 5-ethynyluracil; 5-euD, 5-ethynyluridine; 5-vu, 5-vinyluracil; 5-vuD, 5-vinyluridine; WT, wild-type; 3xUPRT, triple mutant uracil phosphoribosyltransferase (*Toxoplasma gondii*); UMPS, uridine monophosphate synthase

## REFERENCES

- (1) Wei, J.-W.; Huang, K.; Yang, C.; Kang, C.-S. Non-Coding RNAs as Regulators in Epigenetics. *Oncol. Rep.* **2017**, *37* (1), 3–9.
- (2) Richardson, G. M.; Lannigan, J.; Macara, I. G. Does FACS Perturb Gene Expression? *Cytometry* **2015**, *87* (2), 166–175.
- (3) Pfister, G.; Toor, S. M.; Sasidharan Nair, V.; Elkord, E. An Evaluation of Sorter Induced Cell Stress (SICS) on Peripheral Blood Mononuclear Cells (PBMCs) after Different Sort Conditions - Are Your Sorted Cells Getting SICS? *Journal of Immunological Methods* **2020**, *487*, 112902.
- (4) Singha, M.; Spitalny, L.; Nguyen, K.; Vandewalle, A.; Spitale, R. C. Chemical Methods for Measuring RNA Expression with Metabolic Labeling. *WIREs RNA* **2021**, *12* (5), 1650.
- (5) Nguyen, K.; Fazio, M.; Kubota, M.; Nainar, S.; Feng, C.; Li, X.; Atwood, S. X.; Bredy, T. W.; Spitale, R. C. Cell-Selective Bioorthogonal Metabolic Labeling of RNA. *J. Am. Chem. Soc.* **2017**, *139* (6), 2148–2151.
- (6) Zajackowski, E. L.; Zhao, Q.-Y.; Zhang, Z. H.; Li, X.; Wei, W.; Marshall, P. R.; Leighton, L. J.; Nainar, S.; Feng, C.; Spitale, R. C.; Bredy, T. W. Bioorthogonal Metabolic Labeling of Nascent RNA in Neurons Improves the Sensitivity of Transcriptome-Wide Profiling. *ACS Chem. Neurosci.* **2018**, *9* (7), 1858–1865.
- (7) Paredes, E.; Das, S. R. Click Chemistry for Rapid Labeling and Ligation of RNA. *ChemBioChem.* **2011**, *12* (1), 125–131.
- (8) Nainar, S.; Cuthbert, B. J.; Lim, N. M.; England, W. E.; Ke, K.; Sophal, K.; Quechol, R.; Mobley, D. L.; Goulding, C. W.; Spitale, R. C. An Optimized Chemical-Genetic Method for Cell-Specific Metabolic Labeling of RNA. *Nat. Methods* **2020**, *17* (3), 311–318.
- (9) Nguyen, K.; Kubota, M.; Arco, J. del; Feng, C.; Singha, M.; Beasley, S.; Sakr, J.; Gandhi, S. P.; Blurton-Jones, M.; Fernández Lucas, J.; Spitale, R. C. A Bump-Hole Strategy for Increased Stringency of Cell-Specific Metabolic Labeling of RNA. *ACS Chem. Biol.* **2020**, *15* (12), 3099–3105.
- (10) Kubota, M.; Nainar, S.; Parker, S. M.; England, W.; Furche, F.; Spitale, R. C. Expanding the Scope of RNA Metabolic Labeling with Vinyl Nucleosides and Inverse Electron-Demand Diels–Alder Chemistry. *ACS Chem. Biol.* **2019**, *14* (8), 1698–1707.
- (11) Suzuki, K.; Tsunekawa, Y.; Hernandez-Benitez, R.; Wu, J.; Zhu, J.; Kim, E. J.; Hatanaka, F.; Yamamoto, M.; Araoka, T.; Li, Z.; Kurita, M.; Hishida, T.; Li, M.; Aizawa, E.; Guo, S.; Chen, S.; Goebel, A.; Soligalla, R. D.; Qu, J.; Jiang, T.; Fu, X.; Jafari, M.; Esteban, C. R.; Berggren, W. T.; Lajara, J.; Nuñez-Delgado, E.; Guillen, P.; Campistol, J. M.; Matsuzaki, F.; Liu, G.-H.; Magistretti, P.; Zhang, K.; Callaway, E. M.; Zhang, K.; Belmonte, J. C. I. In Vivo Genome

Editing via CRISPR/Cas9 Mediated Homology-Independent Targeted Integration. *Nature* **2016**, *540* (7631), 144–149.

(12) Minn, A. J.; Gupta, G. P.; Siegel, P. M.; Bos, P. D.; Shu, W.; Giri, D. D.; Viale, A.; Olshen, A. B.; Gerald, W. L.; Massagué, J. Genes That Mediate Breast Cancer Metastasis to Lung. *Nature* **2005**, *436* (7050), 518–524.

(13) Azevedo-Pouly, A. C. P.; Elgamil, O. A.; Schmittgen, T. D. RNA Isolation from Mouse Pancreas: A Ribonuclease-Rich Tissue. *JoVE* **2014**, *90*, 51779.

(14) Satelli, A.; Li, S. Vimentin in Cancer and Its Potential as a Molecular Target for Cancer Therapy. *Cell. Mol. Life Sci.* **2011**, *68* (18), 3033–3046.

## Recommended by ACS

### Probing Nascent RNA with Metabolic Incorporation of Modified Nucleosides

Mrityunjay Gupta, Robert C. Spitale, *et al.*

SEPTEMBER 08, 2022  
ACCOUNTS OF CHEMICAL RESEARCH

READ 

### Exploiting Endogenous Enzymes for Cancer-Cell Selective Metabolic Labeling of RNA in Vivo

Samantha Beasley, Robert C. Spitale, *et al.*

APRIL 13, 2022  
JOURNAL OF THE AMERICAN CHEMICAL SOCIETY

READ 

### Live-Cell RNA Imaging with Metabolically Incorporated Fluorescent Nucleosides

Danyang Wang, Ralph E. Kleiner, *et al.*

AUGUST 05, 2022  
JOURNAL OF THE AMERICAN CHEMICAL SOCIETY

READ 

### Complete Chemical Synthesis of Minimal Messenger RNA by Efficient Chemical Capping Reaction

Naoko Abe, Hiroshi Abe, *et al.*

MAY 24, 2022  
ACS CHEMICAL BIOLOGY

READ 

Get More Suggestions >